

# Electron Glass Dynamics

Ariel Amir, Yuval Oreg, Yoseph Imry

*Department of Condensed Matter Physics,*

*Weizmann Institute of Science, Rehovot, 76100, Israel*

**Keywords:** Aging, Slow relaxations, Glasses, Coulomb interactions

Examples of glasses are abundant, yet it remains one of the phases of matter whose understanding is very elusive. In recent years, remarkable experiments have been performed on the dynamical aspects of glasses. Electron glasses offer a particularly good example of the 'trademarks' of glassy behavior, such as aging and slow relaxations. In this work we review the experimental literature on electron glasses, as well as the local mean-field theoretical framework put forward in recent years to understand some of these results. We also present novel theoretical results explaining the periodic aging experiment.

## Contents

<b>I. Introduction</b>	3
<b>II. Why a logarithm?</b>	4
A. Activated processes	4
B. Tunneling processes	5
<b>III. Aging experiments</b>	6
A. Aging protocols	6
1. Indium Oxide	8
2. Granular Aluminum	10
3. Other materials	10
B. TRM in electron glasses	11
C. Generalized IRM (periodic protocol)	11
<b>IV. Why is full aging observed and when does it fail?</b>	12

	2
A. Local mean field approach	12
1. Properties of the relaxation matrix $A$	14
2. IRM protocol - theory	15
3. Generalized IRM (periodic protocol) - theory	17
B. Noise in electron glasses	18
1. Why $1/f$ noise occurs?	18
<b>V. Memory in electron glasses</b>	20
A. Anomalous field effect	20
B. Two-dip experiments	21
<b>VI. How electron glasses remember - theoretical picture</b>	23
A. Connection between the conductance and the occupation number relaxations	23
1. Miller-Abrahams resistor network	24
2. Variable Range Hopping	25
3. Coulomb gap	25
B. Why the conductance increases out-of-equilibrium : Coulomb gap	26
C. Why the conductance increases out-of-equilibrium : long time relaxations	27
D. Anomalous field effect and two-dip experiments - qualitative theory	29
E. Estimating the timescales	33
<b>VII. Future prospects</b>	34
<b>VIII. Acknowledgements</b>	34
<b>References</b>	34

## I. INTRODUCTION

Slow relaxations in nature have been observed long ago, in many contexts. Two important examples are the ‘stretched exponential’ behavior experimentally observed by Kohlrausch in the 19th century, when studying discharge in a certain electrostatic setup known as a Leiden jar [1] and mechanical relaxations in silk threads, used by Weber [2] to hang his magnets in his seminal works on magnetism.

Slow relaxations are also important signatures of glassy behavior: the Vogel-Fulcher law [3] states that the timescale for the thermalization of a glass diverges at a finite temperature. When valid, this temperature is the phase-transition to the glassy phase, below which non-ergodic behavior occurs: the system does not equilibrate, and some states are never visited. Slow relaxations have been known to occur in magnetic materials known as spin glasses [4–7], vortices in superconductors in the glassy phase [8], and in the electron glass system, to name but a few.

In many cases in nature the slow relaxations are logarithmic, over several decades in time. These systems range from flux relaxation in superconductors [9], through crumpling paper [10] where the volume is measured as a function of time, as well as biological systems such as plant rheology[11], and electron glasses which we will focus on here. One should note that it is not trivial to distinguish a logarithm from a stretched exponential: one has to go to short time scales, where the power-law behavior of the stretched exponential is distinctly different from logarithmic. For this reason relaxations in the electron glass were initially erroneously reported as stretched exponential. Fig. 1 demonstrates a logarithmic relaxation after a sudden change in the voltage of a gate coupled to the sample.

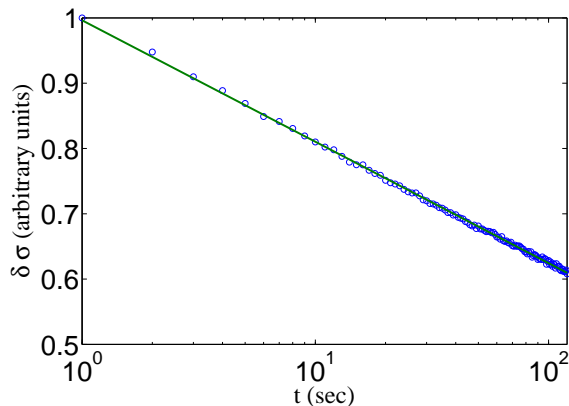


FIG. 1: Demonstration of a logarithmic relaxation in electron glasses, after a sudden change in gate voltage. In some cases, the logarithmic change in conductance can be measured from times of order of seconds to several days [12]. Data courtesy of Z. Ovadyahu.

In this review we shall explain how one can understand these slow, logarithmic relaxations in electron glasses via the use of a local mean-field approximation, and also extend this to various aging protocols, in which the response of the system to a perturbation depends also on the time the perturbation was applied for. We describe the experimental details, but only briefly discuss theoretical frameworks other than the local mean-field approach.

The structure of the manuscript is as follows. We first explain different mechanism leading to a broad distribution of relaxation times, which will give rise to logarithmic relaxation over a broad range. We review the different experimental protocols demonstrating aging, and their results, focusing on granular aluminum and InO. We then go on to describe the local mean-field approach, and compare its prediction with the experimental results. We discuss the possible relation between  $1/f$  noise and logarithmic relaxations. Next, more involved protocols related to memory effects in the system are reviewed, and the necessary theoretical framework for a qualitative understanding of them is given. We conclude with our view regarding the important, open questions in this field.

## II. WHY A LOGARITHM?

One may decompose the logarithmic relaxation into a weighted sum of decaying exponentials, by taking an inverse Laplace transform. This gives a distribution of relaxation rate which is  $P(\lambda) = c/\lambda$ , with  $c = 1/\log(\lambda_{\max}/\lambda_{\min})$ , with  $\lambda_{\max}$  and  $\lambda_{\min}$  the upper and lower cutoffs of the distribution. Notice that the distribution of the logarithm of  $\lambda$  is uniform between the lower and upper cutoffs. Indeed, taking its Laplace transform of  $P(\lambda)$  yields, for times  $1/\lambda_{\max} \ll t \ll 1/\lambda_{\min}$  [13]:

$$\int e^{-\lambda t} P(\lambda) d\lambda \equiv L(t) = -\gamma_E - \log(\lambda_{\min} t), \quad (1)$$

with  $\gamma_E$  the Euler constant. Notice that the upper cutoff does not enter the expression, but the lower one does.

In order to understand the logarithmic relaxations, it is sufficient to understand how a distribution  $P(\lambda) = C/\lambda$  arises. This is the purpose of the next section.

### A. Activated processes

The simplest way to obtain a broad  $1/\lambda$  distribution, is via thermally activated processes: let us assume that a particle hops between trapped states, and that the distribution of the energy barriers between two adjacent traps is uniformly distributed in the interval  $[E_{\min}, E_{\max}]$ ,  $P(E) = \frac{1}{E_{\max} - E_{\min}}$ . If we assume thermally activated processes,

the rate  $\lambda$  associated with a given barrier is given by the Arrhenius law,  $\lambda \sim e^{-E/T}$  (throughout the manuscript  $k_B \equiv 1$ ). Calculating the distribution of the rates, we find that  $P(\lambda)d\lambda = P(E)dE$ , and therefore  $P(\lambda) \sim T/\lambda$ .

In various experiments [14–16] the temperature dependence was shown to be much weaker, if at all measurable. For these cases, this rules out the possibility of the above mechanism as being responsible for the slow relaxations, and opts for a quantum mechanism, nearly independent of temperature. Quantum tunneling is the natural process to look at, in order to avoid the strong dependence on temperature.

## B. Tunneling processes

If we look at a particle hopping between localized states, the tunneling rate is exponential in the distance  $r$  (up to polynomial corrections). If we assume that the spatial distribution of localized states is uniform, we can readily calculate the distribution of hopping rates between a given site and its nearest-neighbor: the rate  $\lambda \sim e^{-r/\xi}$ , where  $\xi$  is the localization length, taken here as a constant for simplicity. We have  $P(\lambda)d\lambda = P(r)dr$ , with  $P(r)$  the probability distribution of having the nearest-neighbor at a distance  $r$ . It is easier to calculate the cumulative of this distribution, *i.e.*, the probability  $C(r)$  that all neighbors are more than a distance  $r$  away from a given site. The probability of a given site to be more than a distance  $r$  away is  $p = 1 - V_d r^d / L^d$ , with  $V_d = \pi^{d/2} / \Gamma(d/2 + 1)$  the volume of a  $d$  dimensional unit sphere and  $L$  the system size. Thus,  $C(r) = p^N$ , where  $N$  is the number of sites. In the limit  $N \gg 1$ , this can be simplified to give:

$$P(r) = \frac{dV_d}{\langle r \rangle} [r/\langle r \rangle]^{d-1} e^{-V_d [r/\langle r \rangle]^d}, \quad (2)$$

$\langle r \rangle = \frac{L}{N^{1/d}}$  being the average nearest-neighbor distance.

This immediately gives:

$$P(\lambda) = \frac{dV_d \xi / \langle r \rangle}{\lambda} [-\xi \log(\lambda) / \langle r \rangle]^{d-1} e^{-V_d [-\xi \log(\lambda) / \langle r \rangle]^d}. \quad (3)$$

Thus, we see that this mechanism yields a  $1/\lambda$  distribution, up to logarithmic corrections, which may be of importance if the relaxation is probed over enough decades in time. Related analysis leading to approximately logarithmic relaxations was made in Refs. [17–19], where the relaxation rate was assumed to be the exponential of a smoothly distributed variable.

Ref. [20] analyzes this problem more carefully, and finds the exact distribution of relaxation rates, for any spatial dimensions, in the low density limit. It is shown that the resulting distribution is approximately  $P(\lambda) \sim 1/\lambda$ , but in

dimensions higher than one there are logarithmic corrections similar to those of Eq. (3), but with different numerical coefficients. The real-space renormalization group method used also allows to find the structure of the eigenmodes, which show interesting localization properties: all eigenmodes are localized, but with size diverging as one goes to vanishing eigenvalues, as  $\sim e^{C|\log^d(-\lambda/2)|}$ , with  $C$  a constant. In one dimension, for example, this would yield a power-law relation.

An interesting and relevant question addresses the issue of how this picture is changed when one considers tunneling not only of a single particle, but simultaneous quantum tunneling of a number of electrons [21–28]. Obviously, the associated timescales would be longer, since now one has to replace  $e^{-r/\xi}$  by  $e^{-\sum_j r_j/\xi}$ , where  $r_j$  are the tunneling distances of each of the particles involved in the many-particle tunneling process. In principle there are many possibilities to connect the initial and final states, but the one where the sum over distances is minimal would be the dominant one. There should be quantitative changes in the form of  $P(\lambda)$ , namely, in the corrections to the numerator of Eq. (3). Since estimating the numbers for single-particle processes (see section (VIE)) yields too short relaxation times, we are led to believe that these processes must be considered. A step in that direction was taken in Ref. [29]. However, the temperature dependence which they estimate is not consistent with the rather temperature independent results discussed above. In our view, the question of many-particle tunneling still deserves further attention.

### III. AGING EXPERIMENTS

The first experiments showing slow relaxations in the electron glass were performed by Monroe *et al.* [30] in 1987, who looked at the time-dependence of the capacitance of a sample of GaAs, after injection of excess charge.

Later, Ovadyahu and collaborators have shown remarkable aging behavior (a concept to be shortly explained) in a series of extensive experiments done mainly on InO samples, in a field effect transistor setup [12, 14, 15, 17, 19, 31]. In the following, we review the basic experimental procedure used in the experiments, and clarify a common confusion between two different kinds of aging experiments used by the scientific community. We then go on to review the existing theoretical models used to explain the results.

#### A. Aging protocols

Aging is the general phenomenon related to a relaxation which depends on the 'age' of the system: in some experiments, the system is quenched to a low temperature phase at time  $t = 0$ , and the response  $R$  of the system

to a perturbation applied at time  $t_w$  is tested at time  $t$ . If  $R$  depends explicitly on both  $t$  and  $t_w$ , and is not only a function of  $t - t_w$ , the system is referred to as "aging" over time, since its properties are not translationally invariant with respect to time.

Indeed, experiments done on spin glasses [4–7] have shown such "aging" behavior. In this context, the above protocol is known as a thermoremanent magnetization (TRM) experiment.

Another protocol, which we will focus on, follows the following procedure, illustrated in Fig. 2:

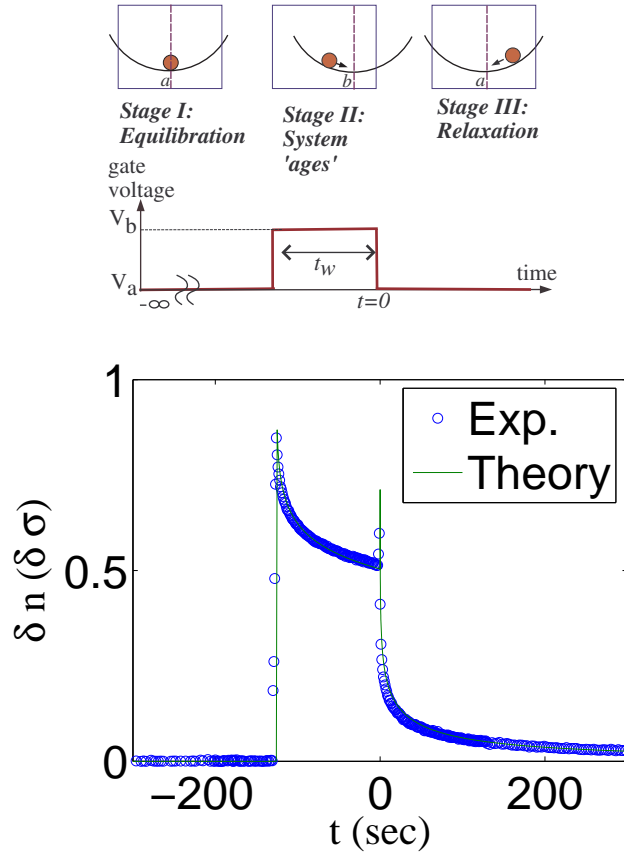


FIG. 2: A schematic description of the different stages of the IRM aging protocol, taken from Ref. [32]. The lower part shows the experimental result (circles), courtesy of Z. Ovadyahu, and theoretical predictions of the model (solid line), discussed in section (IV). Stage II of the experiment shows exactly the same experimental data as Fig. 1, *i.e.*, at this stage the conductance relaxes logarithmically with time. In stage III, the relaxation turns out to depend only on the ratio  $t/t_w$ .

1) The system is let to equilibrate for a long time  $t_1$  at the low temperature phase (not necessarily reaching the true equilibrium).

2) A perturbation is applied for a time  $t_w$ .

3) A time  $t$  after the perturbation has been switched off, the physical observable  $f(t, t_w)$  is measured.

It is important to note that in practice, in most cases the system does not fully equilibrate during the first stage, and in that case this timescale can have implications on the observables in later stages.

The main experimental result for electron glasses are as follows: During stage II, the relaxation is well described by a logarithm, while in stage III excellent data collapse is obtained when time is rescaled according to  $t_w$ , in other words, the relaxation  $f(t, t_w)$  in fact only depends on the ratio  $t/t_w$ .

In the spin glass context, this type of experiment is known as an isothermal remanent magnetization (IRM) experiment. Fig. 3 illustrates schematically the two protocols described above (TRM and IRM), as well as two other protocols which will be discussed later on.

In a sense, the IRM experiment is much simpler, since the system is presumably close to equilibrium at all times during the experiment, provided the perturbation is small such that we are in the linear-response regime. Recently, it has been suggested that calling this type of experiment an aging experiment is misleading, exactly for this reason [33] (since this experiment does not show that the system properties depend on the time from the thermal quench). As we shall later see, understanding the slow relaxations also for this experiment is actually quite involved, and presents some unsolved questions.

We shall now review the experimental results obtained for the different systems.

### 1. Indium Oxide

Pioneering experiments using the above *IRM* protocol, in the context of electron glasses, have been performed mainly on Indium Oxide, by Ovadyhau *et al.* In Ref. [14] they show that "full" (also called simple) aging is obtained: the function  $f(t, t_w)$  depends only on the ratio  $t/t_w$ , *i.e.*,  $f(t, t_w) = g(t/t_w)$ . For short times, they observe that the function  $g(t/t_w)$  depends on the logarithm of its argument. These properties will be elucidated in the next subsection. It turns out that this is by no means an accident related to the peculiar properties of InO, and occurs also for various other systems. Qualitatively similar results are obtained for crystalline samples and amorphous samples, demonstrating the broad applicability of the results. Ref. [19] discusses the deviations of  $f(x)$  from a logarithmic dependence, and also observe deviations from full aging for large enough gate voltages. In Ref. [12], Orlyanchik *et al.* use the same protocol but perturb the system by an electric field (which they termed 'stress aging'), and not a gate voltage. This did not modify the full aging behavior, for not too large fields.

Fig. 4 demonstrates this scaling behavior for a number of cases discussed in the following, by showing data collapse



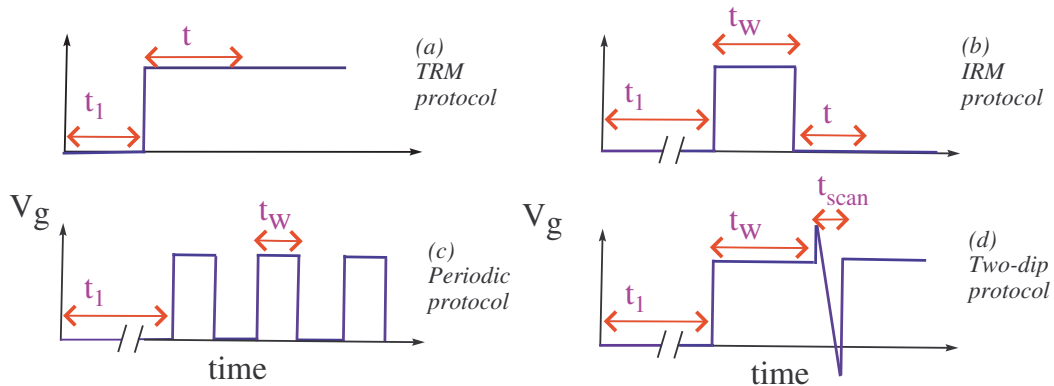


FIG. 3: Schematic illustration of different protocols in use, relating to the aging and memory effects in electron glasses. In all protocols, at a given time (the crossing point of the  $x$  and  $y$  axis, in the figure), the temperature is quenched to reach the glass phase. (a) describes the TRM protocol, only recently performed in the context of electron glasses [33], but extensively used in spin glass experiments [4–7]. In this protocol, one waits a time  $t_1$ , and perturbs the system (in the electron glass, typically by changing the gate voltage). A time  $t$  later, the response of the system (*i.e.*, the conductance) is measured. If  $t_1 \gg t$ , one obtains a logarithmic relaxation of the conductance, for times  $t$  smaller than the cutoff  $1/\lambda_{\min}$  of the relaxation rate distribution. Such a relaxation is shown in Fig. 1. The important point, however, is that generally one can also consider  $t_1 < t$ , which distinguishes this from the IRM protocol. The measured conductance will depend explicitly on both variables  $t_1$  and  $t$ , and in a non-trivial way, which is not well understood. (b) describes the IRM protocol, in which  $t_1$  is assumed much larger than other experimental timescales involved (in typical experiments, it is of the order of a day). After the time  $t_1$  one changes the gate voltage, for a duration  $t_w$  (the ‘waiting-time’). A time  $t$  after the gate voltage is returned to its initial value, the conductance is measured. Here, the ratio  $t/t_w$  can be much smaller or much larger than unity, as long as both are still small compared to  $t_1$ . Fig. 2 shows the experimental results of a typical experiment, and a curve showing the theoretical prediction. The theoretical analysis for this protocol is performed in section (IV A 2). (c) describes a generalization of this, where a periodic square pulse gate voltage is applied, and the conductance is measured throughout the experiment. Unlike most systems, here the response to a periodic signal is not periodic, since the whole experiment is essentially still in the transient period, before the periodic regime is maintained. Fig. 5 shows the result of such an experiment. The relevant theoretical analysis is performed in section (IV A 3). It is assumed that  $t \ll t_1$ . (d) describes the two-dip protocol: here, the gate voltage is changed at some time, and the system begins to relax logarithmically to its equilibrium. A time  $t$  later, a scan of conductance versus gate voltage is made. It turns out that as the system equilibrates at some gate voltage  $V$ , it ‘digs’ a dip in conductance at this gate voltage. In this protocol a new dip begins to form at the new gate voltage, as the old one is erased over time, which gives the protocol its name. The protocol is used to demonstrate the memory effects, and also to quantify the timescales involved. It is described in section (VB), and analyzed qualitatively from the theoretical point of view in section (VID). Also here it is assumed that  $t \ll t_1$ .

when the time axis is rescaled by  $t_w$ . The theoretical curve will be discussed in section (IV).

## 2. Granular Aluminum

Extensive experimental work using the above *IRM* protocol has been performed on granular Aluminum by Grenet *et al.* [16, 34]. Most of the results show striking similarity to those obtained for InO, see Fig. 4. Some differences occur in the behavior of the two-dip experiment, which will be described in section (VB).

## 3. Other materials

Experiments performed on a 2D electron system in silicon by Jaroszyński and Popović have shown slow relaxations and aging [35–37]. They experimentally observe a transition between a phase where aging effects exist (dependence on  $t_w$ ) to one at higher densities where no such dependence exists. In the aging regime, they find full aging only below another critical density. While very interesting by its own right, it seems that the underlying mechanism is

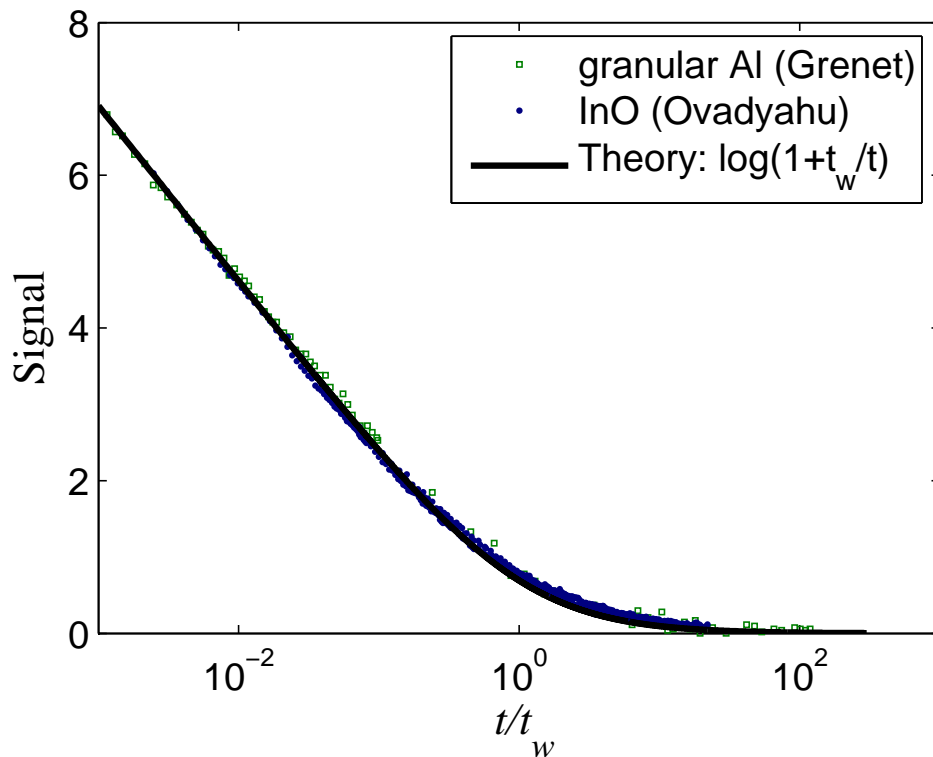


FIG. 4: Comparison between the theoretical prediction of Eq. (17) and various experiments. No fitting parameters are used.

Data courtesy of Z. Ovadyahu and T. Grenet.

different than the one which occurs for InO and Al, which is the one we focus on in this review, and therefore we shall not elaborate on this extensive set of experiments. Borini et *al.* [38] did observe full aging in porous silicon, at room temperature, which seems to fit the theoretical framework that we shall put forward in section (IV), see Fig. 4.

In the group of A. Goldman, experiments performed on thin films of bismuth or lead showed logarithmic relaxations in the conductance after a change in gate-voltage, which relaxed to a different conductance value, depending on the value of the gate voltage [39]. They also observed an anomalous field effect [40], which will be discussed in section (7). It would be interesting to see the behavior of this system when the IRM protocol is applied.

Recent experiments have shown that Nickel samples can also exhibit slow relaxations, with behavior which seems to be similar to that of granular Aluminum and InO [41]. In this case, however, a transition between a ferromagnetic state and a super paramagnetic state seems to have a substantial effect on the relaxation rates. As a result, the magnetic field has a striking effect on the relaxation times. Future experimental and theoretical work in this direction looks promising.

### B. TRM in electron glasses

In a recent experiment Grenet et *al.* have extended the above protocol to the case when the system is only partially equilibrated before the measurement sequence is performed [33]. This adds another timescale to the problem  $t_1$ , the time from the temperature quench to the first voltage step, as shown in Fig. 3(a). The above IRM protocol is the case where  $t_1 \gg t_w$ . It turns out that for smaller  $t_1$ , the measurements depend on it. Remarkably, a 'superposition principle' akin to that observed in spin glasses [42] is still maintained: the response to two voltage pulses is the sum of the responses to each of the them independently. This has not been explained theoretically, for the spin glass nor the electron glass, and would be an interesting subject for future research.

### C. Generalized IRM (periodic protocol)

Another protocol that comes to mind is the generalization of the IRM protocol to deal with an arbitrary series of pulses. An elegant experiment is discussed in Ref. [43], where the sample has been subjected to a periodic sequence of square pulses, see Fig. 3(c). Unlike the common scenario, where the response to a periodic signal is also periodic, after a short transient, here, the whole experiment is found in the transient period. Fig. 5 shows the result of the experiment, together with the theoretical prediction, which will be derived and explained in section (IV A 3).

#### IV. WHY IS FULL AGING OBSERVED AND WHEN DOES IT FAIL?

It is the purpose of this section to present the theoretical models explaining the aging behavior, and the limitations to obtaining full aging.

##### A. Local mean field approach

In a pioneering work, Thouless, Anderson and Palmer introduced the TAP equations, to deal with the equilibrium properties of spin glass [44]. A similar approach was used in Ref. [45], to deal with the statics of the Coulomb glass problem. It was shown that by using a local mean-field approach (which retains the individual identity of each site - not averaging over the disorder), one obtains the Coulomb gap, a soft gap in the density-of-states discussed in section (VIA 3). The long range nature of the problem gives rise to a large number of effective neighbors a given electron interacts with, which gives intuitive justification for the use of the mean-field approach. This was quantified in various works [46–48], indicating that the relevant criterion for the validity of the mean-field is that the power  $\alpha$  characterizing decay of the interaction  $1/r^\alpha$  should be small enough. The results suggest that for Coulomb interactions in two-dimensions and above one could use the local mean-field approach.

In Ref. [49], the local mean-field approach was extended to treat the dynamical aspects.

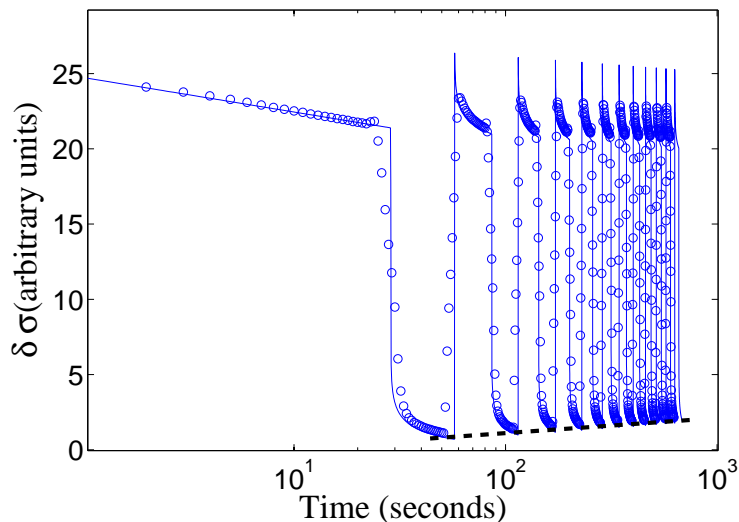


FIG. 5: Comparison between the theoretical analysis of section (IV A 3) (solid line) and an experiment (circles) where the sample is subjected to a periodic perturbation. The dashed line demonstrates the logarithmic increase of the baseline, see Eq. (21). No fitting parameters are used. Data courtesy of Z. Ovadyahu.

The equations describing the dynamics are:

$$\frac{dn_i}{dt} = \sum_{j \neq i} (\gamma_{ji} - \gamma_{ij}), \quad (4)$$

with the rates given by Fermi's golden rule[50]:

$$\gamma_{ij} \sim |M_q|^2 \nu f_i (1 - f_j) e^{-\frac{r_{ij}}{\epsilon}} [1 + N(\Delta E)], \quad (5)$$

where  $f_i$  is the Fermi-Dirac distribution,  $\Delta E$  is the energy difference before and after the tunneling event,  $\nu$  is the phonon density-of-state,  $M_q$  is the corresponding matrix element and  $N(\Delta E)$  is the Bose-Einstein function. For upward transitions ( $E_j > E_i$ ) the square brackets are replaced by  $N(\Delta E)$ . These rates may be renormalized due to polaron-type orthogonality effects [51], which were suggested to be of importance in electron glasses [52].

The Bose-Einstein function expresses the underlying assumption that the phonons thermalize fast and are found in thermal equilibrium.  $\Delta E$  is the energy difference between the two sites, which is affected by the Coulomb interactions with all other sites, *i.e.*,  $\Delta E = E_j - E_i$ , with:

$$E_i = \epsilon_i + \sum_{j \neq i} \frac{e^2 f_j}{r_{ij}}. \quad (6)$$

It should be emphasized that in this local mean-field approach the sites are not assumed to be equivalent, as is clearly seen by the implicit site indices. This is very different than other mean-field approaches to the electron glass problem [53–56].

A characteristic of glasses is the abundance of metastable states, with energies close to that of the true ground state [57]. Also in this case, there are many metastable states, *i.e.*, electronic configurations for which all the time derivatives (the LHS of Eq. (4)) vanish. This has not been investigated systematically within this framework, although it would be interesting to do so. A numerical investigation of the energy landscape has been performed in a related model through Monte-Carlo simulations, by Baranovskii *et al.*, where the metastable states were coined "pseudo ground states" [58]. For recent related works see 59, 60.

Close enough to a *particular* metastable state characterized by an electron configuration  $\vec{n}_0$ , one can linearize the equations of motion for  $\delta \vec{n} \equiv \vec{n} - \vec{n}_0$ :

$$\frac{d\delta \vec{n}}{dt} = A \delta \vec{n}, \quad (7)$$

where the off-diagonal matrix  $A$  is given by the expression [49]:

$$A_{ij} = \gamma_{ij}^0 \frac{1}{n_j^0(1-n_j^0)} - \sum_{k \neq j,i} \frac{e^2 \gamma_{ik}^0}{T} \left( \frac{1}{r_{ij}} - \frac{1}{r_{jk}} \right), \quad (8)$$

with  $\gamma_{ij}^0$  the equilibrium rates obeying detailed balance, see Eq.(5).

The diagonal matrix elements are given by  $A_{ii} = -\sum_{j \neq i} A_{ij}$ , guaranteeing particle number conservation. The matrix is real but not hermitian, due to the  $n_j(1-n_j)$  term. In section (IV B 1) we shall give a very natural explanation for the explicit form of  $A$ , related to the properties of the noise via the Onsager relations [61]:

$$A = \gamma\beta, \quad (9)$$

where  $\gamma$  is a symmetric matrix describing the transition rates at equilibrium, see Eq. (5), and with the diagonal defined such that the sum of columns vanishes, and  $\beta$  is a symmetric matrix whose inverse gives the equilibrium (equal-time) correlation function between two given sites:

$$\beta_{ij} = \frac{\delta_{ij}}{n_i^0(1-n_i^0)} + \frac{1}{T} e^2 / r_{ij}. \quad (10)$$

While  $A$  is not symmetric, its eigenvalues are nevertheless real: this can be seen using Eq. (9) [61]. Near a stable minimum, the eigenvalues must be negative [49], and their distribution will determine the relaxation properties.

### 1. Properties of the relaxation matrix $A$

In section (II B), the statistics of nearest-neighbor distances was analyzed, and was shown to be distributed as  $P(\lambda) \sim 1/\lambda$  up to logarithmic corrections, due to the exponential nature of the tunneling processes. Looking at the matrix  $A$  of the previous section, we find that the off-diagonal matrix elements also decay exponentially in the distance. A numerical study made in Ref. [49] showed that in spite of the more involved form of the matrix elements (related to the energy dependence), the above property is still retained. Considering the toy-model where this energy dependence of the matrix elements is neglected (which is physically correct when the localization length is small enough, but is not always the case in experiments), one obtains a random-matrix class which is defined as follows:

1.  $A_{ij} = e^{-r_{ij}/\xi}$ .
2.  $A_{ii} = -\sum_{j \neq i} A_{ij}$ .

As mentioned earlier, the second property arising directly from particle conservation number.

A heuristic approach to understand qualitatively the emerging distribution of relaxation rates was made in Ref. [49]. Later, an *exact* solution was found, in the low-density case [20], which confirms the numerical result described above: up to logarithmic corrections which depend on the dimensionality and may be of importance if the experimental resolution is fine enough, the leading order behavior is a uniform distribution of the *logarithm* of the relaxation rate, *i.e.*,  $P(\lambda) \sim 1/\lambda$ . This will play a key role in the understanding of the IRM protocol, to be described next.

## 2. IRM protocol - theory

In Ref. [32], the  $P(\lambda) \sim 1/\lambda$  distribution was the starting point of an analysis of the IRM protocol. An underlying assumption is that the state of the system can be described by a vector  $\delta\vec{n}$ , describing the deviation from an equilibrium or metastable state, and that the evolution in time is given by:

$$\frac{d\delta\vec{n}}{dt} = A\delta\vec{n}. \quad (11)$$

Notice that although the above equation is identical to Eq. (7), which was derived from the mean-field approach, here we take a more general approach, where this equation is the starting point. The distribution mentioned above is that of the eigenvalues of the matrix.

The crux of the matter is that when a gate-voltage, for example, is changed, the equilibrium point changes, say from  $\vec{n}_a$  to  $\vec{n}_b$ , such that the system is instantaneously thrown out of equilibrium. Relaxation to the new equilibrium is excitation with respect to the initial equilibrium. Fig. 2 describes the different stages of the experiment schematically.

It is clear that in the stage II, the system is relaxing back to its new equilibrium, so that in terms of the eigenmodes its deviation from equilibrium can be written as:

$$\vec{n}(t) = \vec{n}_b + \sum_q c_q \vec{b}_q e^{-\lambda_q^b(t+t_w)}, \quad -t_w < t < 0, \quad (12)$$

where  $\lambda_q^b$  are the relaxation rates of the relaxation matrix  $A$  at point  $B$ ,  $\vec{b}_q$  are the eigenvectors, and  $c_q$  are the weights of the decomposition into eigenmodes.

Let us assume that the modes contribute, on average, positively and uniformly to the conductance  $\sigma(t)$ , *i.e.*:

$$\delta\sigma \sim \sum_{\lambda} |A_{\lambda}|, \quad (13)$$

where  $|A_{\lambda}|$  is the amplitude of the mode  $\lambda$  in the decomposition of  $\vec{n}(t) - \vec{n}_b$  into eigenmodes. This is a central point which will be discussed in section (VIB). We obtain that:

$$\delta\sigma(t) \sim \sum_q e^{-\lambda_q^b(t+t_w)}, \quad -t_w < t < 0. \quad (14)$$

For the large time window  $1/\lambda_{\max} \ll t \ll 1/\lambda_{\min}$ , this gives a logarithmic relaxation:

$$\delta\sigma(\tilde{t}) \sim -\gamma_E - \log[\tilde{t}\lambda_{\min}], \quad (15)$$

with  $\gamma_E$  is the Euler constant, and  $\tilde{t} = t_w + t$  is the time from the *first* change in gate voltage, obviously independent of  $t_w$ .

Similarly, in stage III, the relaxation is described by:

$$\vec{n}(t) = \vec{n}_a + \sum_q c_q \vec{a}_q (e^{-\lambda_q^b t_w} - 1) e^{-\lambda_q^a t}. \quad (16)$$

An equivalent sum was given heuristically by Grenet *et al.* [16].

For the IRM protocol, we finally obtain after summing up the series in the same manner as that done to obtain Eq. (15) [32]:

$$\delta\sigma(t, t_w) \propto \log(t + t_w) - \log(t) = \log(1 + t_w/t). \quad (17)$$

Fig. 4 shows the correspondence of this to the experimental results in 3 different electron glasses.

We are now in a position to understand why full aging occurs within this model: in general, Eq. (16) predicts a functional dependence on the parameters  $t$  and  $t_w$  of the form  $g(t+t_w) - g(t)$ . For the specific underlying distribution of relaxation rate, it was shown that  $g(x)$  is logarithmic, which leads to the full aging of Eq. (17). It can be shown that the converse is also true, and that  $P(\lambda) \sim 1/\lambda$  (associated with a logarithmic  $g(x)$ ) is the *only* distribution which will give rise to full aging.



It is important to note that in the above analysis it was assumed that the system was initially in equilibrium. As mentioned, in practice it is possible that the system did not fully equilibrate in the first stage of the experiment, and in that case the reciprocal equilibration time  $1/t_1$  (see Fig. 3) will replace  $1/\lambda_{\min}$ .

### 3. Generalized IRM (periodic protocol) - theory

It is possible to extend the IRM protocol, to the case where a more complex sequence of pulses is used. A natural choice is a periodic sequence of pulses, *i.e.*, the system state is switched from one value of gate voltage to another, after a  $t_w$  length of time. Such a protocol was carried out in detail in Ref. [43], as discussed in section (III C). We shall now give a theoretical analysis of the experiment, in the same fashion as was done in the previous section:

At every instance in time, the system relaxes to its current equilibrium, which we shall denote by  $A$  or  $B$ , depending on the current value of the gate voltage. Every time the gate voltage is switched from  $A$  to  $B$ , the vector  $\delta\vec{n}$  gains an extra  $\Delta\vec{n}$ . Similarly, when the voltage is switched from  $B$  to  $A$ , the gain is  $-\Delta\vec{n}$ .

Thus, for example, a time  $t$  after *two* cycles of gate voltage changes, the state of the system is described by:

$$\vec{n}(t) = \vec{n}_a + \sum_q c_q \vec{a}_q [1 - e^{\lambda_b t_w} (e^{-\lambda_q^b t_w} - 1) e^{-\lambda_q^a t_w}] e^{-\lambda_a t}. \quad (18)$$

Assuming, as before, that points  $A$  and  $B$  are close enough such that we can neglect the difference in the eigenmodes and eigenvalues, the sum can be readily evaluated to give:

$$\delta\sigma \sim \log[1 + t_w/(t + 2t_w)] + \log[1 + t_w/t]. \quad (19)$$

Writing out the sum explicitly for a general sequence of pulses, we find the following simple rule: the contribution of a step up is  $\log[\lambda_{\min}(t - t_{step})]$ , and the contribution of step down is  $-\log[\lambda_{\min}(t - t_{step})]$ . Indeed, for the IRM protocol we obtain  $\log(\lambda_{\min}(t_w + t)) - \log(\lambda_{\min}(t)) = \log(1 + t_w/t)$ .

Looking at the system state a time  $t$  after  $N$  pulses, its conductance is given by:

$$\delta\sigma \sim \sum_{j=0}^N (-1)^{j+1} \log[t + t_w(2j - 1)] - \log[t + t_w(2j - 2)]. \quad (20)$$

To sum up the sequence, it is helpful to sum subsequent pairs of switches. Looking at the contribution of a pair of switches occurring a time  $t \gg t_w$  earlier, it contributes  $\log(1 + t_w/t) \sim t_w/t$ . Therefore the response after  $N \gg 1$

pulses is given approximately by:

$$\sum_{j=1}^N t_w/(2jt_w) = \log(N)/2 = \log[t/(2t_w)]/2. \quad (21)$$

The fact that this series diverges is profound: it means that we will have approximately periodic signal, but with a baseline that diverges logarithmically in time. This is exactly what is demonstrated in Fig. 5, comparing the evaluation of Eq. (20), with no fitting parameters, with experiments .

The striking result of this analysis, confirmed by the experiment, is that while we are used to systems responding periodically to a periodic perturbation after a short transient (e.g: RCL circuits, mechanical systems etc.), here, the system remains in the 'transient' period for the whole duration of the experiment.

## B. Noise in electron glasses

$1/f$  noise occurs in many physical [62, 63], as well as biological and economic systems [64, 65]. Electron glasses are no exception, and various experimental studies have measured  $1/f$  noise in such systems [66–72]. An even larger amount of work has been invested in the theoretical aspects of this problem. The pioneering works of Shklovskii [73] were later followed by various other approaches [29, 74–79]. In a recent work [61], the mean-field framework has been shown to yield a  $1/f$  noise in the site occupancies, which has not been measured until now, but being a local object is a much simpler property than the conductance noise.

In the following, we shall shortly explain the relation between the slow relaxations extensively discussed earlier, and the  $1/f$  noise. We note that the correspondence to the experimental data should be done with extra care: since  $1/f$  is so common, the experimental observation of such noise by itself is by no means a confirmation that the electron glass mechanism yielding this noise is the dominating one, and additional signatures must be considered.

### 1. Why $1/f$ noise occurs?

Although noise is measured at equilibrium, Onsager understood in a seminal work that it is generically related to the way a system returns to equilibrium after a slight perturbation [80].

In the following, we shall show how this Onsager principle relates the logarithmic relaxations discussed earlier to the noise in the system.

*Onsager's regression hypothesis* [81] states that the *equation of motion* of the correlation function  $\phi_{ij}(t) = \langle \delta n_i(t) \delta n_j(t) \rangle$  is obtained by simply replacing  $\delta n_i(t)$  in the equation of motion (11) by the function  $\phi_{ij}(t)$ :

$$\frac{d\phi_{ij}(t)}{dt} = A_{ik}\phi_{kj}(t). \quad (22)$$

To find the correlation function one also needs the initial conditions:

$$\phi_{ij}(0) = \langle \delta n_i(0) \delta n_j(0) \rangle \equiv \beta_{ij}^{-1}. \quad (23)$$

To find the matrix  $\beta$ , we write the free energy [45]:

$$F = \sum_i \epsilon_i \tilde{n}_i + \sum_{i \neq j} \frac{e^2 \tilde{n}_i \tilde{n}_j}{r_{ij}} + T \sum_i \left[ \left( \frac{1}{2} + \tilde{n}_i \right) \log \left( \frac{1}{2} + \tilde{n}_i \right) + \left( \frac{1}{2} - \tilde{n}_i \right) \log \left( \frac{1}{2} - \tilde{n}_i \right) \right], \quad (24)$$

with  $\tilde{n}_i \equiv n_i - \frac{1}{2}$ . The local mean-field equations can be obtained from the minimalization condition  $\frac{\partial F}{\partial \tilde{n}_i} = 0$ . Notice that each site contains a positive background charge of  $\frac{1}{2}$ , to keep charge neutrality.

Expanding  $F$  near a metastable state (a local minimum), we have:

$$F = F_0 + \frac{kT}{2} \sum_{i,j} \beta_{ij} \delta n_i \delta n_j, \quad (25)$$

with  $\beta$  given by Eq. (10).

The correlation matrix is proportional to  $\beta^{-1}$ , since we have a quadratic free energy:

$$\langle \delta n_i \delta n_j \rangle = (\beta^{-1})_{ij}. \quad (26)$$

Regardless of the question of determining the noise spectrum, which we shall shortly derive, at this stage we can use another theorem due to Onsager to put the form of the non-hermitian relaxation matrix  $A$  of Eq. (8) in a more natural context: the Onsager symmetry principle states that  $A\beta^{-1}$  must be a symmetric matrix. Indeed, in our case  $A = \gamma\beta$ , with  $\gamma_{ij}$  the equilibrium current between sites  $i$  and  $j$ , as was mentioned in section (IV A).

Let us proceed to the calculation of the noise spectrum. After finding  $\beta$ , we can solve Eq. (22), and obtain the noise spectrum of the average site occupancy [61]. This leads to the expression:

$$\phi_{ii}(\omega) = \sum_{\alpha} \frac{1}{\beta_{ii}} |\psi_i^{\alpha}|^2 \frac{2\lambda_{\alpha}}{\omega^2 + \lambda_{\alpha}^2}, \quad (27)$$

where  $\psi_i^\alpha$  describes the amplitude of the  $\alpha$ 'th eigenmode of the relaxation matrix  $A$ . The factor  $\frac{1}{\beta_{ii}}$  describes the physically clear fact that only sites with energies close to the Fermi-energy will contribute to the noise, since they are "soft" and their occupancy fluctuates significantly. We therefore find that:

$$\langle\langle \delta n^2 \rangle\rangle_\omega \sim \frac{1}{N} \sum_{\alpha,i} \frac{\frac{2}{\lambda_\alpha}}{1 + (\frac{\omega}{\lambda_\alpha})^2}, \quad (28)$$

where  $\langle\langle ; \rangle\rangle$  denotes averaging over sites as well as time.

Plugging in the  $P(\lambda) \sim 1/\lambda$  distribution of rates, we finally obtain the noise spectrum:

$$\langle\langle \delta n^2 \rangle\rangle_\omega \sim \frac{1}{N} \int_{\lambda_{\min}}^{\lambda_{\max}} d\lambda \frac{\frac{1}{\lambda^2}}{1 + (\frac{\omega}{\lambda})^2} = \frac{1}{N\omega} \int_{\frac{\lambda_{\min}}{\omega}}^{\frac{\lambda_{\max}}{\omega}} dm \frac{1}{1 + m^2}. \quad (29)$$

This shows that for  $\lambda_{\min} \ll \omega \ll \lambda_{\max}$ , a  $1/f$  spectrum indeed follows for the noise in the average occupation number.

## V. MEMORY IN ELECTRON GLASSES

### A. Anomalous field effect

There is a clear experimental demonstration that for electron glasses perturbing the system causes the conductance to increase. In 'ordinary' field effect transistors, where interactions are not as strong, adding charge carriers to the system by changing a gate voltage (see Fig. 6), will increase the conductance, and taking charge away will make it decrease. In electron glasses, however, after full or partial equilibration, changing the charge carriers number in any direction will make the conductance *increase*. This surprising property is called the anomalous field effect [82]. It is clear that the only thing which distinguishes the particular value of gate voltage used is the fact that the system was let to equilibrate in it. Moreover, it is clear that performing the experiments 'quasi-statically', waiting a long enough time at each voltage point, will retrieve the normal field effect. Thus, the voltage scan rate must enter. Fig. 7 demonstrates the results of scanning at different rates. Intuitively, relaxing to lower in energy (deeper) metastable states should indeed result in a lower conductance. The theoretical framework for understanding this property will be given in section (VID).

The width of the dips (also referred to as cusps) is an important characteristic of the system: an elaborate set of experiments [83] have shown that the cusp shape does not depend on the scan rate (for scan rates varying over 3

decades), and is independent on disorder and magnetic field. As such, it manifests an intrinsic property of the system, which has also been shown to be correlated with the interaction strength (by showing a strong density dependence)[84].

We now go on to describe a slightly more involved experimental protocol, that can serve as a useful characterization tool to probe changes in the system timescales.

### B. Two-dip experiments

An important protocol for demonstrating and quantifying the memory effects in electron glasses in a striking way was developed by Ovadyahu et al. [84, 85]. The experimental protocol is as follows (see also Fig. 3):

1. As in the anomalous field effect, the system is let to equilibrate for a long time ( $t_1$  in Fig. 3), typically of the order of day or several days. The gate voltage is fixed at a value  $V_1$  during this time.
2. At time  $t = 0$ , the gate voltage is changed to a value  $V_2$ .
3. A time  $t_w$  later, a scan of conductance vs. gate voltage is made.

Clearly, if  $t_w = 0$ , we observe the anomalous field effect mentioned earlier. However, for finite values of the waiting-time  $t_w$ , the system exhibits a striking memory effect: while the dip at the original gate voltage  $V_1$  is gradually erased, a new dip begins to form at the gate voltage  $V_2$ . For this reason this important protocol is termed the 'two-dip experiment'. Fig. 8 shows the result of a typical experiment.

At some time  $t_w$ , the two dips will be equal in magnitude. This provides a natural experimental time  $\tau$  characterizing

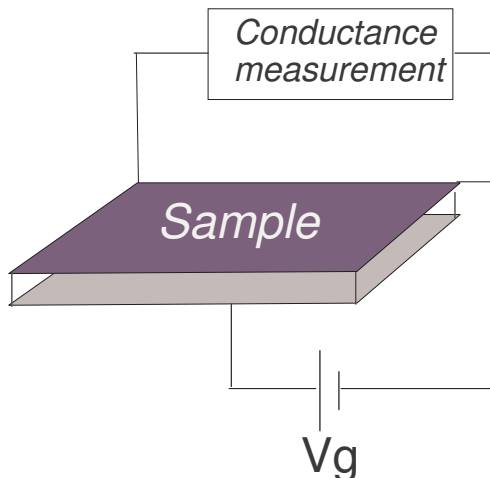


FIG. 6: Schematic illustration of the field effect transistor setup. A gate voltage is attached to the sample via a separator, and the conductance of the sample is measured while changes in the gate voltage charge the sample, positively or negatively.

the system. Experimentally, Ref. [15] demonstrates that this timescale can be consistently measured in various other ways: for example, one may change the value of the gate voltage when the system is close to equilibrium, and measure how long it takes for the (logarithmic) change in conductance to decay to half its value at one second. We will discuss the physical significance of these timescales in section (VID), and show why the two approaches give similar results.

In Ref. [52], the temperature dependence of this timescale was carefully measured. The result appears to be quite counter-intuitive: as the temperature increases, and one may expect the dynamics to be faster,  $\tau$  actually increases. This was associated with a quantum effect, reminiscent of the anomalous temperature effect which occurs in the dynamics of the spin-boson problem for coupling to an Ohmic bath and for a certain regime of parameters [86]. However, applying a theory constructed for a two level system to one as complex as electron glass is possibly an oversimplification, and this point requires further theoretical attention. Furthermore, one should make sure that the

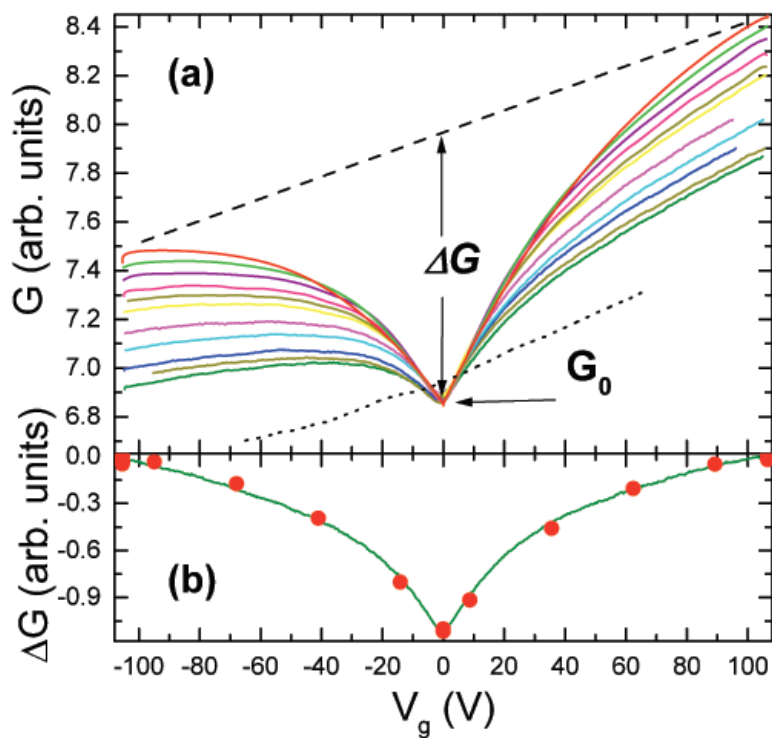


FIG. 7: The dependence of the conductance on the gate voltage was checked for various scan rates, in a typical field effect transistor setup (see Fig. 6). In addition to a linear trend, related to the "normal" field effect, there is a surprising symmetric component, whose amplitude depends on the scan rate (a). Subtracting the linear trend and normalizing the amplitude, the rate dependence is eliminated (b). Figure taken from Z. Ovadyhau, PRB 78, 195120 (2008) with permission from the author.

measured timescale is indeed an intrinsic timescale of the system, not associated with  $t_1$ , as mentioned in section (III A).

A subtle but important difference between the experiments done on InO and those on granular aluminum [16, 34], relates to the evolution in time of the plateaus outside the dips (cusps). While in InO these are static in time, in granular aluminum they show a logarithmic dependence on time as well. Recently, T. Grenet and J. Delahaye showed this could be consistently understood in terms of metallic screening in the thin films [87].

## VI. HOW ELECTRON GLASSES REMEMBER - THEORETICAL PICTURE

### A. Connection between the conductance and the occupation number relaxations

So far we discussed the relaxations of the occupation numbers. One still has to explain how this influences the conductance, which is a much more involved property. Namely, in the analysis we assumed that the relaxation modes contribute positively to the conductance. Experimentally, it is indeed clear that the conductance is raised when the system is perturbed out of equilibrium. However, it is not obvious theoretically, a-priori, why any perturbation of the

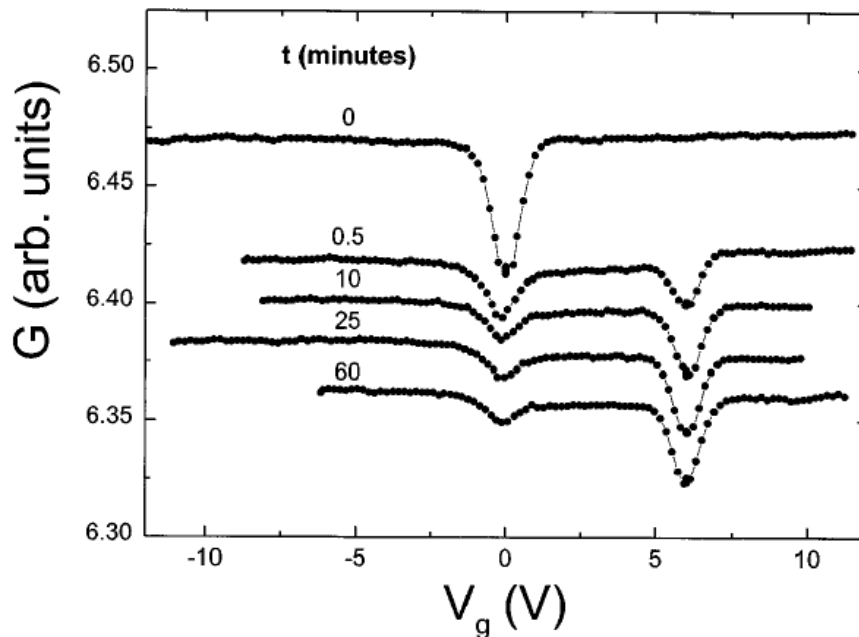


FIG. 8: A typical experimental measurement for the two-dip experiment protocol. Initially, the anomalous field effect accounts for the dip at zero gate voltage, at which the system was equilibrated. The gate voltage is then shifted to a different value, and as the system equilibrates a new dip begins to form at the new value while the initial one is slowly erased. Figure taken from A. Vaknin, Z. Ovadyahu and M. Pollak, PRL 81, 669 (1998) with permission from the author.

occupancies will tend to raise it. Ref. [88] shows how this can come about for a non-interacting electronic systems (in addition to giving experimental results). In the following, we shall give two explanations of this remarkable property, where the interactions play a central role. Before that, we shortly review the properties of the equilibrium conductance, which will be important for the discussion which follows.

### 1. Miller-Abrahams resistor network

In a seminal paper, Miller and Abrahams showed that the conductance of a system of non-interacting electrons, 'hopping' between localized states, can be mapped to the determination of the resistance of a resistor-network, where the value of the resistor between site  $i$  and site  $j$  is given by [50]:

$$R_{ij} = T/[e^2\gamma_{ij}^0], \quad (30)$$

with  $\gamma_{ij}^0$  the equilibrium hopping rate from site  $i$  to site  $j$ , see Eq. (5). Detailed balance, assumed to hold at equilibrium, ensures us that the resistor is well-defined. The intuition behind this is that well coupled sites will have a good conductance between them. As one raises the temperature, the effect on  $\gamma_{ij}$  is exponential, and exceeds the linear term in the numerator. For a mesoscopic sample (or for numerical purposes) it might be important to deal with the connections to the leads. Ref. [89] shows how to incorporate them into the same framework, with the result that the resistor between a site and the leads takes the same form as that of Eq. (30). When all the energies involved are much larger than the temperature, the rates  $\gamma_{ij}$  can be shown to take the approximate form [90]:

$$\gamma_{ij} \sim \exp\left[-\frac{2r_{ij}}{\xi} - \frac{|E_i - \mu| + |E_j - \mu| + |E_i - E_j|}{2T}\right], \quad (31)$$

This is commonly used regardless of the above restriction, erroneously. In Refs. [89, 91] it is shown that by taking interactions on the local mean-field level, this formula remains correct, but with  $E_i$  renormalized due to the Coulomb interactions between sites.

Determining the resistance of the complete network is still not an easy task. Extensive work has been done on this problem using percolation theory methods [91], some using the concept of percolation in phase-space [26, 27]. A direct, 'brute force' method is the numerical determination of the resistance, via Monte-Carlo simulations [89]. In the following subsection we show a heuristic approach due to Mott, later extended by Efros and Shklovskii to deal with the interacting problem, that finds the leading order behavior.



## 2. Variable Range Hopping

In 1969, Mott considered the problem of hopping conductance, *i.e.*, the conductance occurring through phonon assisted jumps (hops) between localized states. In a brilliant analysis, Mott realized that at low enough temperatures it is beneficial for the electrons to hop not to the nearest-neighbor, but to neighbors more further away [92]. This is in spite of the exponential-in-distance penalty, in order to reduce the exponential-in-energy penalty. The temperature determines the scale for the exponential-in-energy penalty, and thus at extremely low temperature the electron tunnels over a large distance, to find a site close to it in energy, see Eq. (31). The result is that:

$$\sigma \sim e^{-\left(\frac{T_0}{T}\right)^{-\frac{1}{d+1}}}, \quad (32)$$

where  $d$  is the dimension of the system, and  $T_0 \approx \frac{1}{\nu\xi^d}$ , with  $\nu$  the density-of-states and  $\xi$  the localization length (taking the dielectric constant to be unity).

## 3. Coulomb gap

About 4 decades ago, it was understood that Coulomb interactions can have profound effects on the density-of-states (DOS) of electronic systems near the Fermi energy, namely, leading to the vanishing of the DOS at the Fermi energy [93] and the emergence of a 'soft' gap near it [94], suggested by an analysis by Efros and Shklovskii. Since then, a large number of analytical [28, 54, 56, 91, 95], numerical [96–101] and to a lesser extent experimental [102, 103] approaches have dealt with this interesting problem. The current understanding is that there is a power-law DOS at equilibrium, with exponent depending on the dimensionality. Since it is a direct result of the Coulomb interactions, it is called the Coulomb gap.

For the current work, we shall not attempt to review the literature on the subject. The only ingredient that we shall take away from this for the following, is the existence of a soft-gap near the Fermi energy. Surprisingly, this can also be understood from the local mean-field theory discussed in section (IV A) [45]. In two-dimensions, Ref. [89] shows that the gap obtained by the local mean-field approach is consistent with that predicted by Efros [28] and Raikh [95] by a self-consistent equation approach (taking only single electron transitions into account). Fig. 9 compares this 2D result with the Efros prediction of  $\frac{2|E|}{\pi e^4}$ . It would be worthwhile to show how this comes about by analytically solving the local mean-field equations, which has not been done to this date.

### B. Why the conductance increases out-of-equilibrium : Coulomb gap

It is plausible that when pushed out-of-equilibrium, the Coulomb gap is washed out. It is interesting and experimentally relevant, to ask how the gap is recovered in time. Experimentally, most of the gap would be recovered in very short times, as is analyzed extensively by Tsigankov *et al.* [104]. At long times, there could be two possibilities: the first, is that all metastable states manifest the same Coulomb gap, and that the complete recovery of the Coulomb gap to each of them is a slow process, for energies close to the Fermi energy. This approach was supported by Yu by generalizing the Efros self-consistent approach to the time-dependent domain [105]. The second possibility is that as time goes on, the system probes different metastable states, each of which possesses a slightly different Coulomb gap, which 'deepens' as the systems relaxes by going into deeper (lower in energy) metastable states. Work in this direction was done in Ref. [104].

The idea is now as follows: it is plausible that the DOS near the Fermi energy is crucial for the conductance properties. This was used by Efros and Shklovskii in a seminal work , to show how the Mott picture for variable-range-hopping, briefly discussed in section (VIA 2), should be modified [94]. Although the use of the single particle tunneling DOS in the conductance calculation is not justified [106], their prediction was confirmed in a huge number of experimental systems [107], functionally but not necessarily quantitatively. In a recent work [89], it was shown

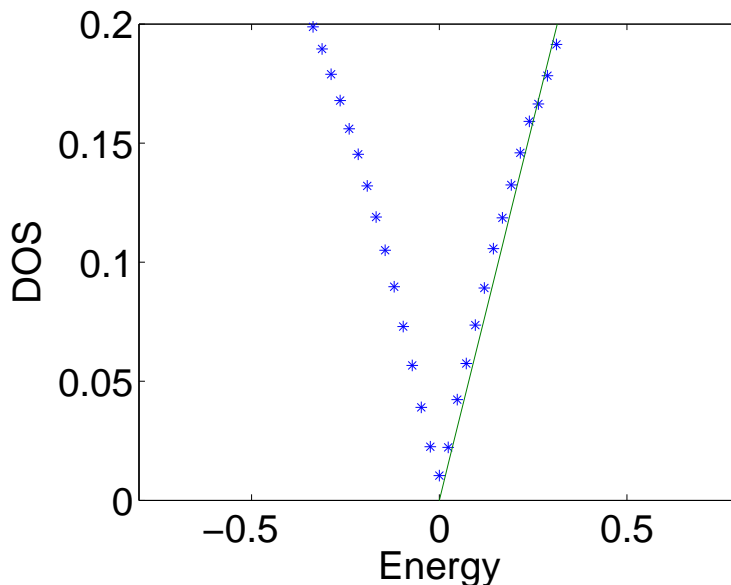


FIG. 9: Comparison between the local mean-field approach [49] and the Efros self-consistent equation approach [28], yielding a linear Coulomb gap (solid line) in two-dimensions, with slope  $\sim \frac{2}{\pi e^4}$ . The figure is taken from Ref. [89].

that by following the local mean-field approach, one can self-consistently take the interactions into account, and essentially verify the Efros-Shklovskii picture. Thus, the Coulomb gap reduces the conductance, by reducing the density of available states near the Fermi energy. The picture that emerges is that through the Coulomb interactions the system 'digs' a hole in the DOS, and makes its own conductance diminish. Therefore, by kicking the system out of equilibrium, we enhance the conductance, as we assumed earlier in the analysis of the IRM protocol, by taking the contribution of the modes to be positive. The problem that remains is the understanding of the timescales: as we mentioned, various references suggest that the Coulomb gap is created on fast timescales of the order of the Maxwell time [91] (although, as mentioned, some works indicate that at energies close to the Fermi energy, *i.e.*, the bottom of the gap, the Coulomb gap takes a long time to form [105]). The next section will give a possible solution, that shows how this effect can be understood on more general ground, beyond the single particle relaxations.

### C. Why the conductance increases out-of-equilibrium : long time relaxations

In the presence of Coulomb interactions, slow relaxing modes can modify the energies of other sites, and thus influence the conductance even if the modes are isolated, and the tunneling between them and the rest of the sites is negligible (since it is exponentially suppressed). This picture also explains why one may talk about an out-of-equilibrium conductance: there can be a separation of timescales between the (relatively quick) equilibration time of the current carrying sites, the 'backbone', and the isolated, slowly relaxing modes outside it. When the slow modes have not equilibrated with the rest of the system, strictly speaking the system is out-of-equilibrium. Nevertheless, there is a well defined conductance that can be experimentally measured, defined by the internally equilibrated sites belonging to the backbone, which have reached quasi-equilibrium in the presence of the slowly changing potential created by the slow modes (*i.e.*, their statistics is described by the Fermi-Dirac distribution). In this sense, the combination of the long ranged Coulomb interactions and the localized modes explains why the conductance returns slowly to its equilibrium value. This is not enough, however, to explain why it does so *monotonically*, as is clearly seen experimentally in the IRM experiment, for example.

In order to understand this, a simple argument has been put forward by Ref. [29]. In the following we give our version of the argument.

An essential ingredient is the separation of timescales between those associated with hopping between sites which contribute significantly to the conduction (by definition "fast" processes), and clusters of sites which support "slow" modes: Ref. [20] shows that isolated clusters lead to an abundance of slow modes with a distribution approximately

given by  $P(\lambda) \sim 1/\lambda$ , but this is not the only mechanism leading to slow modes: Coulomb interactions will give rise to modes related to the tunneling of many electrons, related to the work of Kozub et al. [29]. The contribution of these clusters to the conductance is not negligible, however, since they affect the energies of the sites associated with the fast processes (from now on we refer to these as the "backbone"), through the Coulomb interactions. One might expect that the contribution will be effectively random: sometimes they will give rise to an increase and sometimes a decrease. It turns out that *on average*, however, they give rise to a *positive* contribution. We now go on to the crux of the matter: let us consider a relaxation mode associated with an isolated cluster some distance away from the backbone, as shown in Fig. 10.

Since we have a separation of timescales, it is still justified to think of the Miller-Abrahams resistance network associated with the conduction backbone (see section (VIA 1), which is presumably in equilibrium, but with the energies of the sites in it affected by the current configurations of the slowly relaxing modes outside the backbone, which have not yet fully equilibrated. Let us consider the value of the resistance associated with two close sites on the backbone,  $A$  and  $B$  in Fig. 10. The resistance between them is given by Eq. (31), showing that the dependence on energy is:

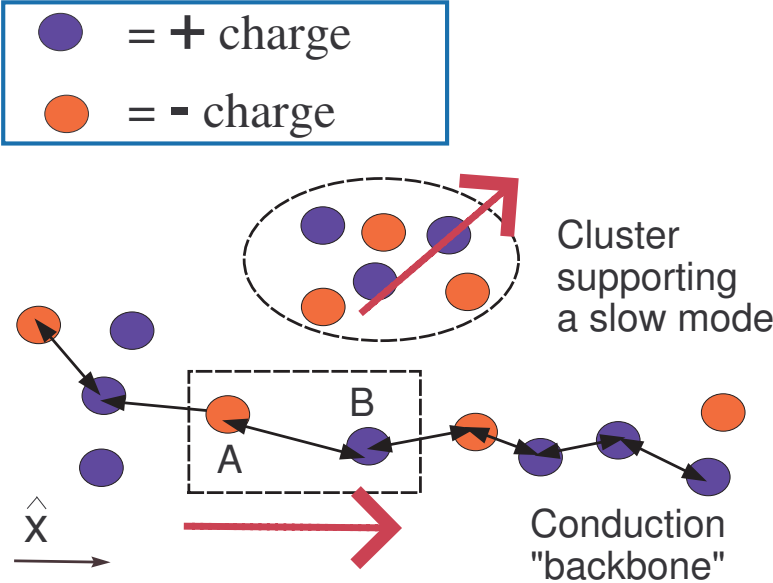


FIG. 10: Schematic illustration used to demonstrate why a relaxation of a mode outside the conduction "backbone" contributes negatively to the conduction, on average. The dotted (purple) arrows denote the dipole moments of the cluster and of two sites in the backbone. These will prefer to point in opposite directions, on the average, and thus while a cluster relaxes it will tend to *raise* the energy difference between the two sites in the backbone, *on average*, thus making the conductance lower.

$$R \sim \exp\left[\frac{|E_A - \mu| + |E_B - \mu| + |E_A - E_B|}{2T}\right] \quad (33)$$

The claim is that modes that relax in energy will tend to make the value of the resistor larger (on average) as they relax. Let us assume that  $E_A < \mu$  and  $E_B > \mu$ . We know that in equilibrium (which is assumed for the sites on the backbone), the average occupations obey Fermi-Dirac statistics [49], therefore we know that site  $A$  is negatively charged and site  $B$  is positively charged. Therefore there is a net dipole moment with a component in the positive  $\hat{x}$  direction, see Fig. 10. On average, it is plausible that there will therefore be a tendency for the dipole moment of the relaxation cluster (encircled by an eclipse in the figure) to be aligned in the  $-\hat{x}$  direction. Therefore, on average, in the relaxation process the cluster will contribute to the electric field in the vicinity of the sites  $A$  and  $B$  in the positive  $\hat{x}$  direction, thus making the energy difference between them larger still, and increasing the resistance of Eq. (33). It is possible that the argument does not rely explicitly on the specific form of the interactions, as long as it is not too short ranged. Thus, it seems like a robust and generic mechanism (albeit, non-rigorous in the form given here) for explaining why the conductance decreases as the system relaxes, which can be used to explain qualitatively some of the experiments described earlier.

#### D. Anomalous field effect and two-dip experiments - qualitative theory

Following the theoretical discussion, we can go back to explain qualitatively the physics behind the anomalous field effect and the two-dip experiment.

It is clear from the argument of section (VIC), that the conductance decreases as the system equilibrates. Already after single particle transitions take place, the Coulomb gap is formed, as discussed in section (VIB) which accounts for most of the reduction in conductance. Nevertheless, as many particle rearrangements take place, the system conductances continues to decrease, which explains the long timescales involved.

What happens when we make a gate voltage scan? Let us consider a "fast" scan, without yet mentioning compared to what. It is clear that at a given point of the scan, the system is nearly at equilibrium with respect to the gate voltage at which it was equilibrated, not at the current value of the gate voltage. Thus, the system is out-of-equilibrium with regard to the current gate voltage, and therefore has an improved conductance. For small changes of gate voltage, such that the system configuration is still approximately in a local minimum (metastable state), this statement is not true: for these, the system is nearly in equilibrium, and the value of the conductance is nearly the lowest one possible.

This explains qualitatively why one obtains an anomalous field effect, without explaining the characteristic scales involved, the dependence of the scan rate, and without considering the normal field effect which will give an additive linear dependence to the anomalous effect.

It should be emphasized that the Coulomb gap gives intuition of how interactions diminish the conductance of the system, but looking at the time scales involved it is more plausible that it is formed "immediately" at each point of the scan, and that the anomalous field effect is due to more than single particle transitions (as mentioned earlier, Ref. [104] shows that the Coulomb gap due to single electron tunneling forms in very short times).

Let us proceed to the explanation of the two-dip experiment, described in section (VB), which is relatively straightforward on the qualitative level once the anomalous field effect is understood. If we make a gate voltage scan immediately after the gate voltage is changed to its new value, clearly we are still measuring the anomalous field effect, since the system did not change its configuration yet. The result of a scan made after a very long time is also clear: the system will equilibrate at the new gate voltage, and we will measure an anomalous field effect shifted to the new value of gate voltage. Thus, over time the initial dip must slowly vanish, and a new one must begin to form. It turns out experimentally that in many cases there is a symmetry between the depth of the new dip formed and the amplitude by which the old dip has become smaller. This can be readily understood based on the results of section (IV A 2): in a two-dip protocol, the system is initially in equilibrium, and then the gate voltage is changed to a new value. Let us assume a quick scan is made after time  $t_w$ . If we take from this scan only one value, the conductance at the new gate voltage  $V_2$ , which is exactly the position of one of the two dips, we obtain a similar dependence to that of the IRM protocol on time during stage II of the IRM protocol (the only difference is that here there is an additional perturbation made, during the time of the scan itself,  $t_{scan}$ , which slightly destroys the new dip formed, and has to be accounted for [108]). We therefore find that the new dip is formed with an amplitude growing logarithmically in time. Let us denote by  $t_{dip}$  the time it takes to scan the width of the cusp. Therefore measuring the conductance at the old gate voltage in the two-dip experiment is approximately equivalent to the IRM protocol in Stage III, with a relevant time of the order of  $t_{dip}$ : this is the time the system effectively had to dig the gap at  $V_1$ . Thus, the result should be  $\log(1 + t_w/t_{dip})$ , and for  $t_w \gg t_{dip}$  the formation of the new dip and the erasure of the old one both scale as  $\log(t_w)$ , which accounts for the symmetry described above. Now we are in a position to understand the timescale involved in the two-dip experiment, mentioned in section (VB): the requirement that the dips are of the same depth reduces to the equation:

$$|\log(\tau/t_{dip})| = \log(\tau/t_{dip}) = |\log(\lambda_{\min}\tau) - \log(t_{scan}/t_{dip})| = -\log(\lambda_{\min}\tau t_{dip}/t_{scan}), \quad (34)$$

where the term  $-\log(t_{scan}/t_{dip})$  accounts for the reduction of the new dip formed due to the scan.

This finally leads to the relation:

$$\tau \sim \sqrt{\frac{t_{scan}}{\lambda_{\min}}}. \quad (35)$$

Typically,  $t_{scan}$  is of the order of tens of seconds [84]. Thus measuring a value of  $\tau$  of the order of 1000 seconds implies an associated timescale  $1/\lambda_{\min}$  of about a day. This is possibly due to the finite amount of time the system was let to equilibrate prior to the experiment, and not the true cutoff of the underlying distribution.

Before continuing with the two-dip experiment, it is useful to discuss now another way of measuring this timescale, which experimentally leads to similar results [15], and we shall show that it is also consistent theoretically: in this method, one changes the gate voltage, and then simply waits until the conductance deviation decays to its half value from that measured *after one second*.

The procedure is demonstrated in Fig. 11

Here, the analysis is straightforward: according to Eq. (14) the decay in this procedure goes as  $-\gamma_E - \log(\lambda_{\min}t)$ , thus, the normalized decay is:

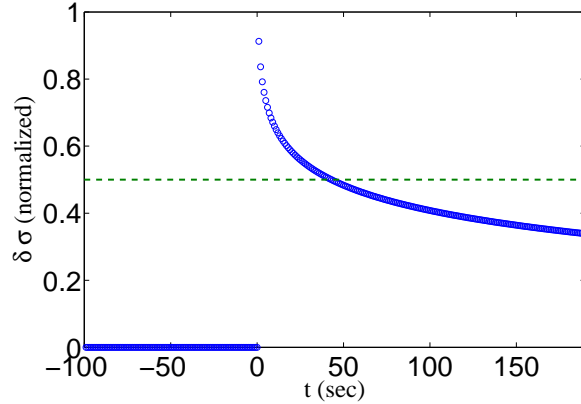


FIG. 11: Illustration of one of the procedures that can be used to determine the timescale of the system: the system is let to equilibrate for a long time, after which a sudden change in gate voltage is made. The signal (conductance change) is normalized to unity at  $t = 1$  second, and the time at which the (logarithmically relaxing) conductance reaches the value of half defines the timescale of the system. Eq. (35) shows the physical significance of this timescale.

$$\frac{\delta\sigma(t)}{\delta\sigma(t = 1\text{sec})} = \frac{-\gamma_E - \log(\lambda_{\min}t)}{-\gamma_E - \log(\lambda_{\min})}. \quad (36)$$

Equating this to 1/2, we find that:

$$\tau \sim \sqrt{\frac{1\text{sec.}}{\lambda_{\min}}}. \quad (37)$$

Clearly, due to the choice of normalization after *one second*, similar to the value  $t_s$ , the two methods qualitatively agree.

Let us return to the two-dip experiment. The theory described in section (IV A 3) might hint that one can use linear response to understand also the two-dip protocol: if the response to a generic period sequence of square pulses can be decomposed into a superposition of contributions arising from the changes in gate voltage, *i.e.*,  $\delta\sigma(t) \sim \int G(t-t') \frac{dV}{dt}(t')$ , where  $G(t-t')$  is a function describing the response of the system to a step function in gate voltage, why not plug in a more complicated dependence of gate voltage on time,  $V(t)$ , to understand two-dip experiments quantitatively? This approach is incorrect, due to a fundamental reason: the dependence on gate voltage is not linear. For square pulses, only two values of gate voltage play a role, and therefore the assumption of linearity is unnecessary, which is why the analysis of section (IV A 3) is correct. But for the two-dip experiment, if we are interested in the values of the conductance associated with other values of gate voltage than  $V_1$  or  $V_2$ , we cannot use this linear response equation.

Therefore within the framework of the  $1/\lambda$  relaxation rate distribution we cannot explain quantitatively the shape of the dips, as well as other interesting questions regarding it, e.g: What determines their dependence temperature and disorder?

Various works have addressed these questions, which we briefly mention now. The general physical picture presented here is similar to that of Refs. [29, 109] with regard to the mechanism leading to the decrease of the conductance and the anomalous field effect, which is the basis for understanding (qualitatively) the two-dip experiment. Ref. [110] suggests that the slow relaxing modes are not (as was assumed above) an intrinsic part of the electronic system, but rather, atomic configurations which change over time and interact with the electronic configuration. Ref. [29], by the same authors, explain that the same mechanism would also be consistent with an intrinsic picture, similar to that described here, and refer to a specific subset of relaxation modes, with a definite structure in space, which they refer to as "chessboard cluster". These were introduced by the same authors in Ref. [111] in order to explain the  $1/f$



noise which occurs in electronic glasses, which we discuss in section (IV B 1). Ref. [112] also deals with the two-dip experiment, but focuses more on the dependence of the dip on temperature, carrier density and disorder, and less on the timescales associated with the formation of the phenomenon.

### E. Estimating the timescales

So far we have mainly discussed the functional form of the relaxations involved, but have not demonstrated why the long time cutoffs of the underlying distribution exceed the experimental timescales involved (which can be hours and days). In fact, this remains a difficult question, for which no clear cut answer exists. While many theoretical mechanisms that can give rise to such slow relaxations exist, it is not clear what distinguishes the slow relaxations described in the previous section, on Anderson insulators and granular systems, and various experiments performed on semiconductors, for which the experimental results are different, and no slow relaxations with full aging is observed. An experimental clue in the direction of solving this profound problem is given by Ref. [84], suggesting that the electron density plays a role in determining the system relaxation time. Indeed, the electronic density in doped semiconductors below the metal-insulator transition does not reach the values of indium oxide. Recent experiments on semiconductors shows that these systems may also exhibit rich behavior and non-exponential relaxations, albeit on much shorter timescales [113]. Measuring the density dependence of the relaxation timescales involved might shed new light on this problem. For the indium oxide samples, on the other hand, it would be good to check experimentally if for the low-density samples one can see a deviation from the clean logarithmic relaxations, signalling that we are nearing the cutoff of the relaxation rate distribution. An idea suggested by Ovadyhau [52] emphasized the effect of Anderson orthogonality catastrophe is slowing down the rate: indeed, experiments suggest that the slow relaxation regime corresponds to that where more than a single electron is present in a localization volume [31, 114]. Another ingredient which may be important for understanding the source of the slow relaxations is the simultaneous tunneling of more than one electron [21–29, 115, 116]. However, such many-particle tunneling events can be present also in semiconductors: one has to show that their significance depends on a parameter which is different in the two systems - a natural candidate is the ratio of the localization length to the average nearest-neighbor distance. This criterion is equivalent to the above mention criterion of having many particles in a localization. Showing this systematically by analyzing the statistics of the many-particle tunneling processes would be a significant step.

## VII. FUTURE PROSPECTS

In this review we discussed the current experimental and theoretical understanding of the memory and aging associated with electron glasses. Throughout, a number of open questions, mostly theoretical, were mentioned. Perhaps the most fundamental regards the timescales associated with the relaxations. What is the role of many particle transitions in determining it? How many electrons tunnel simultaneously? Does the Anderson Orthogonality Catastrophe (or a Franck-Condon type effect) play a substantial role?

Another deep question regards the basic ingredients needed to observe the form of aging and slow relaxations discussed in this review. Experiments performed on spin glasses, for example, show more complex aging behavior [7, 117]. It is in our opinion a worthwhile question to understand the similarities and differences between these two related systems. Structural glasses also show similar behavior [118], which should be further explored.

More technical questions, to which at present we do not have a full answer, regard the quantitative understanding of the two-dip experiment (section (VB)). Also, the TRM protocol described in section (IIIB) still has to be explored further.

Altogether, it seems that electron glasses still pose many more questions and challenges, and prove a useful platform for investigating glassy behavior.

## VIII. ACKNOWLEDGEMENTS

It is our pleasure to thank J. Delahaye, T. Grenet, M. Müller, Z. Ovadyahu, M. Palassini and M. Pollak for illuminating discussions and for useful comments regarding the manuscript. We also thank J. Delahaye, T. Grenet and Z. Ovadyahu for providing us with their experimental data. This work was supported by a BMBF DIP grant as well as by ISF and BSF grants and the Center of Excellence Program.

- 
- [1] R. Kohlrausch, *Ann. Phys.* **12**, 393 (1847).
  - [2] W. Weber, *Ann. Phys.* **34**, 247 (1835).
  - [3] H. Vogel, *Z. Phys.* **22**, 645 (1921); G. S. Fulcher, *J. Am. Ceram. Soc.* **8**, 339 (1925).
  - [4] L. Lundgren, P. Svedlindh, P. Nordblad, and O. Beckman, *Phys. Rev. Lett.* **51**, 911 (1983).
  - [5] R. V. Chamberlin, *Phys. Rev. B* **30**, 5393 (1984).
  - [6] M. Alba, M. Ocio, and J. Hammann, *Europhys. Lett.* **2**, 45 (1986).

- [7] G. F. Rodriguez, G. G. Kenning, and R. Orbach, Phys. Rev. Lett **91**, 037203 (2003).
- [8] X. Du *et al.*, Nature Physics **3**, 111 (2007).
- [9] A. Gurevich and H. K upfer, Phys. Rev. B **48**, 64776487 (2001).
- [10] K. Matan, R. B. Williams, T. A. Witten, and S. R. Nagel, Phys. Rev. Lett. **88**, 076101 (2002).
- [11] D. S. Thompson, J. Exp. Bot. **52**, 1291 (2001).
- [12] V. Orlyanchik and Z. Ovadyahu, **92**, 066801 (2004).
- [13] M. Pollak and Z. Ovadyahu, Phys. Stat. Sol. (c) **2**, 283 (2006).
- [14] A. Vaknin, Z. Ovadyahu, and M. Pollak, Phys. Rev. Lett. **84**, 3402 (2000).
- [15] Z. Ovadyahu, Phys. Rev. B **73**, 214208 (2006).
- [16] T. Grenet, J. Delahaye, M. Sabra, and F. Gay, Eur. Phys. J B **56**, 183 (2007).
- [17] A. Vaknin, Z. Ovadyahu, and M. Pollak, Phys. Rev. B **61**, 6692 (2000).
- [18] A. Vaknin, Z. Ovadyahu, and M. Pollak, Phys. Rev. B **65**, 134208 (2002).
- [19] Z. Ovadyahu and M. Pollak, Phys. Rev. B. **68**, 184204 (2003).
- [20] A. Amir, Y. Oreg, and Y. Imry, Phys. Rev. Lett. **105**, 070601 (2010).
- [21] M. Pollak, Phil. Mag. B **50**, 265 (1984).
- [22] M. Mochena and M. Pollak, Phys. Rev. Lett. **67**, 109 (1991).
- [23] K. Tenelsen and M. Schreiber, Phys. Rev. B **52**, 13287 (1995).
- [24] M. L. Knotek and M. Pollak, J. Non-Cryst. Solids **8**, 505 (1972).
- [25] M. L. Knotek and M. Pollak, Phys. Rev. B **9**, 664 (1974).
- [26] A. P erez-Garrido *et al.*, Phys. Rev. B **55**, R8630 (1997).
- [27] A. M. Somoza, M. Ortu no, and M. Pollak, Phys. Rev. B **73**, 045123 (2006).
- [28] A. L. Efros, J. Phys. C: Solid State Phys **9**, 2021 (1976).
- [29] V. I. Kozub, Y. M. Galperin, V. Vinokur, and A. L. Burin, Phys. Rev. B **78**, 132201 (2008).
- [30] D. Monroe *et al.*, Phys. Rev. Lett. **59**, 1148 (1987).
- [31] Z. Ovadyahu, Phys. Rev. B **78**, 195120 (2008).
- [32] A. Amir, Y. Oreg, and Y. Imry, Phys. Rev. Lett. **103**, 126403 (2009).
- [33] T. Grenet and J. Delahaye, Eur. Phys. J. B **76**, 229 (2010).
- [34] T. Grenet, Eur. Phys. J. B **32**, 275 (2003); T. Grenet, Phys. Stat. Sol. (c) **1**, 9 (2004).
- [35] J. Jaroszy nski and D. Popovi c, Phys. Rev. Lett. **96**, 037403 (2006).
- [36] J. Jaroszy nski and D. Popovi c, Phys. Rev. Lett. **99**, 046405 (2007).
- [37] J. Jaroszy nski and D. Popovi c, Phys. Rev. Lett. **99**, 216401 (2007).
- [38] S. Borini, L. Boarino, and G. Amato, Phys. Rev. B **75**, 165205 (2007).

- [39] G. Martinez-Arizala *et al.*, Phys. Rev. B (R) **42**, 670 (1998).
- [40] G. Martinez-Arizala *et al.*, Phys. Rev. Lett. **42**, 1130 (1997).
- [41] A. Frydman, private communications.
- [42] L. Lundgren, P. Nordblad, and L. Sandlund, Europhys. Lett. **1**, 529 (1986).
- [43] Z. Ovadyahu and M. Pollak, Phys. Rev. B **68**, 184204 (2003).
- [44] D. J. Thouless, P. W. Anderson, and R. G. Palmer, Phil. Mag. **35**, 593 (1977).
- [45] M. Grunewald, B. Pohlmann, L. Schweitzer, and D. Wurtz, J. Phys. C: Solid State Phys., **15**, L1153 (1982).
- [46] M. E. Fisher, S. keng Ma, and B. G. Nickel, Phys. Rev. Lett. **29**, 917920 (1972).
- [47] G. Kotliar, P. W. Anderson, and D. L. Stein, Phys. Rev. B **27**, 602 (1983).
- [48] See T. Mori, arXiv:1004.3622 (2010) and references therein.
- [49] A. Amir, Y. Oreg, and Y. Imry, Phys. Rev. B **77**, 165207 (2008).
- [50] A. Miller and E. Abrahams, Phys. Rev. **120**, 745 (1960).
- [51] A. J. Leggett *et al.*, Rev. Mod. Phys. **59**, 1 (1987).
- [52] Z. Ovadyahu, Phys. Rev. Lett. **99**, 226603 (2007).
- [53] A. A. Pastor and V. Dobrosavljevic, Phys. Rev. Lett. **83**, 4642 (1999).
- [54] M. Muller and L. B. Ioffe, Phys. Rev. Lett. **93**, 256403 (2004).
- [55] S. Pankov and V. Dobrosavljević, Phys. Rev. Lett. **94**, 046402 (2005).
- [56] M. Muller and S. Pankov, Phys. Rev. B. **75**, 144201 (2007).
- [57] M. Mezard, G. Parisi, and M. A. Virasoro, *Spin glass theory and beyond* (World Scientific, Singapore, 1987).
- [58] S. D. Baranovskii, A. L. Efros, B. L. Gelmont, and B. I. Shklovskii, J. Phys. C: Solid Slatte Phys. **12**, 1023 (1978).
- [59] A. Pérez-Garrido, M. Ortuño, A. M. Somoza, and A. Díaz-Sánchez, Phys. Stat. Sol. (b) **218**, 25 (2000).
- [60] S. Kogan, Phys. Rev. B. **57**, 9736 (1998).
- [61] A. Amir, Y. Oreg, and Y. Imry, Ann. Phys. (Berlin) **18**, 836 (2009).
- [62] P. Dutta and P. M. Horn, Rev. Mod. Phys. **53**, 497516 (1981).
- [63] M. Weissman, Rev. Mod. Phys. **60**, 537 (1988).
- [64] P. C. Ivanov *et al.*, Chaos **11**, 641 (2001).
- [65] E. W. Montroll and M. F. Shlesinger, Proc. Natl. Acad. Sci. **79**, 3380 (1998).
- [66] R. Voss, J. Phys. C **11**, L923 (1978).
- [67] J. G. Massey and M. Lee, Phys. Rev. Lett. **79**, 3986 (1997).
- [68] D. McCammon *et al.*, phys. stat. sol. (b) **230**, 197 (2002).
- [69] S. Kar *et al.*, Phys. Rev. Lett. **91**, 216603 (2003).
- [70] O. Cohen, Z. Ovadyahu, and M. Rokni, Phys. Rev. Lett. **69**, 3555 (1992).

- [71] V. Orlyanchik, V. I. Kozub, and Z. Ovadyahu, Phys. Rev. B **74**, 235206 (2006).
- [72] S. Bogdanovich and D. Popovic, Phys. Rev. Lett. **88**, 236401 (2002); J. Jaroszynski, D. Popovic, and T. M. Klapwijk, Phys. Rev. Lett. **89**, 276401 (2002); J. Jaroszynski, D. Popovic, and T. M. Klapwijk, Phys. Rev. Lett. **92**, 226403 (2004).
- [73] B. Shklovskii, Solid State Commun. **33**, 273 (1980).
- [74] S. Kogan and B. Shklovskii, Sov. Phys. Semicond. **15**, 605 (1981).
- [75] V. Kozub, Solid State Commun. **97**, 843 (1996).
- [76] S. Kogan, Phys. Rev. B **57**, 9736 (1998).
- [77] B. I. Shklovskii, Phys. Rev. B **67**, 045201 (2003).
- [78] K. Shtengel and C. C. Yu, Phys. Rev. B **67**, 165106 (2003).
- [79] C. C. Yu, phys. stat. sol. (c) **1**, 2528 (2004).
- [80] L. Onsager., Phys. Rev. **37**, 405. (1931).
- [81] L. D. Landau and E. M. Lifshitz, *Statistical Physics*, part 1, chapter 12 (Pergamon, Oxford, 1980).
- [82] See M. Ben-Chorin, D. Kowal, and Z. Ovadyahu, Phys. Rev. B **44**, 3420 (1991); M. Ben-Chorin, Z. Ovadyahu, and M. Pollak, Phys. Rev. B **48**, 15025 (1993) and references within.
- [83] See [31] and references therein.
- [84] A. Vaknin, Z. Ovadyahu, and M. Pollak, Phys. Rev. Lett. **81**, 669 (1998).
- [85] Z. Ovadyahu and M. Pollak, Phys. Rev. Lett. **79**, 459 (1997).
- [86] See Ref. [51], p.43.
- [87] T. Grenet and J. Delahaye, private communications.
- [88] M. Ben-Chorin, Z. Ovadyahu, and M. Pollak, Phys. Rev. B **48**, 15025 (1993).
- [89] A. Amir, Y. Oreg, and Y. Imry, Phys. Rev. B **80**, 245214 (2009).
- [90] V. Ambegaokar, B. I. Halperin, and J. S. Langer, Phys. Rev. B **4**, 26122620 (1971).
- [91] B. Shklovskii and A. Efros, *Electronic properties of doped semiconductors* (Springer-Verlag, Berlin, 1984).
- [92] N. F. Mott, Phil. Mag. **19**, 835 (1969).
- [93] M. Pollak, Discuss. Faraday Soc. **50**, 13 (1970).
- [94] A. L. Efros and B. I. Shklovskii, J. Phys. C **8**, L49 (1975).
- [95] A. A. Mogilyanski and M. E. Raikh, Sov. Phys. JETP **68**, 1081 (1989).
- [96] S. D. Baranovskii, A. L. Efros, B. L. Gelmont, and B. I. Shklovskii, J. Phys. C: Solid State Phys. **12**, 1023 (1979).
- [97] A. Mobius, M. Richter, and B. Dritler, Phys. Rev. B **45**, 11568 (1992).
- [98] J. H. Davies, P. A. Lee, and T. M. Rice, Phys. Rev. Lett. **49**, 758761 (1982).
- [99] J. H. Davies, P. A. Lee, and T. M. Rice, Phys. Rev. Lett. **29**, 42604271 (1982).
- [100] B. Surer *et al.*, Phys. Rev. Lett. **102**, 067205 (2009).

- [101] M. Goethe and M. Palassini, Phys. Rev. Lett. **103**, 045702 (2009).
- [102] J. G. Massey and M. Lee, Phys. Rev. Lett. **75**, 4266 (1995).
- [103] V. Y. Butko, J. F. Ditusa, and P. W. Adams, Phys. Rev. Lett. **84**, 1543 (2000).
- [104] D. N. Tsiganokov, E. Pazy, B. D. Laikhtman, and A. L. Efros, Phys. Rev. B **68**, 184205 (2003).
- [105] C. C. Yu, Phys. Rev. Lett. **82**, 4074 (1999).
- [106] M. Pollak, Phys. Stat. Sol. (c) **5**, 667 (2008).
- [107] See Ref. [10] of [89].
- [108] We thank T. Grenet for pointing this out.
- [109] A. Burin, J. Low Temp. Phys. **100**, 309 (1995).
- [110] A. L. Burin, V. I. Kozub, Y. M. Galperin, and V. Vinokur, J. Phys. C **20**, 244135 (2008).
- [111] A. L. Burin *et al.*, Phys. Rev. B **74**, 075205 (2006).
- [112] E. Lebanon and M. Muller, Phys. Rev. B **72**, 174202 (2005); M. Muller and E. Lebanon, J. Phys. IV France **131**, 167 (2005).
- [113] V. K. Thorsmølle and N. P. Armitage, Phys. Rev. Lett. **105**, 086601 (2010).
- [114] Z. Ovadyahu, X. M. Xiong, and P. W. Adams, Phys. Rev. B (in press).
- [115] M. Pollak, J. Phys. C: Solid State Phys. **14**, 2977 (1981).
- [116] A. Amir, Y. Oreg and Y. Imry, in preparation.
- [117] V. Dupuis *et al.*, Pramana J. of Phys. **64**, 1109 (2005).
- [118] S. Ludwig, P. Nalbach, D. Rosenberg, and D. Osheroff, Phys. Rev. Lett. **90**, 105501 (2003); S. Ludwig and D.D. Osheroff, Phys. Rev. Lett. **91**, 105501 (2003); P. Nalbach, D. Osheroff, and S. Ludwig, J. Low Temp. Phys. **137**, 395 (2004).